











# Injection Locking Properties of an InP-Si<sub>3</sub>N<sub>4</sub> Dual Laser Source for mm-Wave Communications

Luis Gonzalez-Guerrero , Robinson Guzman , Muhsin Ali , Alberto Zarzuelo, Jessica Cesar Cuello , Devika Dass , Colm Browning , *Member, IEEE*, Liam Barry , *Senior Member, IEEE*, Ilka Visscher , Robert Grootjans, Chris G. H. Roeloffzen , and Guillermo Carpintero , *Senior Member, IEEE*

**Abstract**—We for the first time, the optical injection locking (OIL) to a frequency comb of a hybrid InP-Si<sub>3</sub>N<sub>4</sub> dual laser source for high-purity mm-wave generation through optical heterodyning. Key performance parameters of the comb line demultiplexing functionality provided by this source under OIL – such as adjacent-comb-line side mode suppression ratio (SMSR) and locking range – are reported. It is also shown that the amount of free-running drift exhibited by the hybrid lasers (which should be as little as possible to keep them within the locking range) can be minimized by reducing the amount of bias level applied to the heater-based phase actuators present in such lasers. According to the measured drift, locking range and SMSR, these lasers have potential to achieve continuous locking with SMSR levels of more than 45 dB at comb line separations higher than 9 GHz. Successful carrier generation at 93 GHz is demonstrated by locking the two lasers to an optical frequency comb achieving an ultra-stable International Telecommunication Union (ITU)-compliant signal. Both real-time and DSP-aided data transmissions are demonstrated at this frequency achieving data rates of 12.5 and 28 Gbit/s, respectively.

**Index Terms**—Hybrid integration, InP-Si<sub>3</sub>N<sub>4</sub>, microwave photonics, mm-wave, microring resonator, Si<sub>3</sub>N<sub>4</sub>, silicon photonics.

## I. INTRODUCTION

HYBRID photonic integration is gaining more and more momentum as it allows the use of the best substrate material for each functional building block in a photonic integrated

Manuscript received 21 December 2021; revised 22 March 2022 and 11 April 2022; accepted 13 April 2022. Date of publication 11 May 2022; date of current version 21 October 2022. This work was supported in part by the CONEX-Plus Project funded by UC3M and the European Commission through the Marie-Sklodowska Curie COFUND Action H2020-MSCA-COFUND-2017- under Grant 801538, in part by the European Union’s Horizon 2020 Research and Innovation Programme under Grant 871668 (TERAWAY), and in part by SFI under Grants 18/SIRG/5579 and 13/RC/2077 P2. (Corresponding author: Luis Gonzalez Guerrero.)

Luis Gonzalez-Guerrero, Robinson Guzman, Muhsin Ali, Alberto Zarzuelo, Jessica Cesar Cuello, and Guillermo Carpintero are with the Grupo de Optoelectrónica y Tecnología Laser (GOTL), Universidad Carlos III de Madrid, 28911 Leganes, Madrid, Spain (e-mail: lgguerre@ing.uc3m.es; rcguzman@ing.uc3m.es; muali@ing.uc3m.es; azarzuel@pa.uc3m.es; jecesar@ing.uc3m.es; guiller@ing.uc3m.es).

Devika Dass, Colm Browning, and Liam Barry are with the School of Electronic Engineering, Dublin City University, Glasnevin, Dublin 9, Ireland (e-mail: devika.dass2@mail.dcu.ie; colm.browning@dcu.ie; liam.barry@dcu.ie).

Ilka Visscher, Robert Grootjans, and Chris G. H. Roeloffzen are with the LioniX International BV, 7500 Enschede, AL, Netherlands (e-mail: i.visscher@lionix-int.com; r.grootjans@lionix-int.com; c.g.h.roeloffzen@lionix-int.com).

Color versions of one or more figures in this article are available at <https://doi.org/10.1109/JLT.2022.3171080>.

Digital Object Identifier 10.1109/JLT.2022.3171080

circuit (PIC). The hybrid integration of InP and Si<sub>3</sub>N<sub>4</sub> combines the efficient optical gain of the former platform with the ultra-low loss and high-contrast waveguides of the latter, enabling the development of small form factor, low cost, and high volume transceivers. In the past few years, this platform has produced outstanding results in the development of ultra-narrow linewidth lasers [1] and microwave photonic transmitters [2].

A microwave photonics application that has been recently explored in this hybrid platform is mm-wave heterodyne generation [3]. Recent works integrating two InP-Si<sub>3</sub>N<sub>4</sub> lasers on the same chip have shown that, while the two lasers can have very low intrinsic linewidth, the RF beatnote still exhibits a long-term drift due to thermal instabilities [3]. This drift can hinder the use of such a solution on any telecom system due to failing to comply with current regulations on frequency stability [4]. This drift, however, can be eliminated by optical injection locking (OIL) of the two lasers to an optical frequency comb. OIL is a process in which a “slave” laser is synchronized to a “master” laser by injecting light of the latter into the former. When used as the slave laser of an optical frequency comb, a dual-laser PIC acts as a comb demultiplexer (demux) filter with power boosting capabilities. Compared to the alternative approach of using passive filtering together with traveling-wave amplification, optical comb demux based on OIL minimizes the amount of spontaneous emission noise introduced in the system [5].

Whereas demux filters based on OIL have been extensively explored in the InP platform [6]–[11], no studies have been conducted yet in this hybrid platform. A key characteristic that makes the InP-Si<sub>3</sub>N<sub>4</sub> lasers interesting for this functionality is the high  $Q$  factor they exhibit, which directly affects the two most important parameters for comb demux: the side mode suppression ratio (SMSR) of adjacent comb lines and the locking range. It has been theoretically shown that higher  $Q$  factors improve the SMSR but also narrow the locking range [12]. However, for systems with small relative drift between the comb and locked lasers, a narrow locking range may suffice. In this case, lasers with higher  $Q$  can be advantageous over lower- $Q$  lasers as the former can achieve higher SMSR values.

This paper presents experimental results on the OIL of an InP-Si<sub>3</sub>N<sub>4</sub> dual-laser PIC for high-purity optical-heterodyne mm-wave generation. The SMSR characteristics of such lasers when locked to an optical frequency comb as well as their locking range are reported here for the first time. Ultra-stable mm-wave generation at 93 GHz is demonstrated by locking the

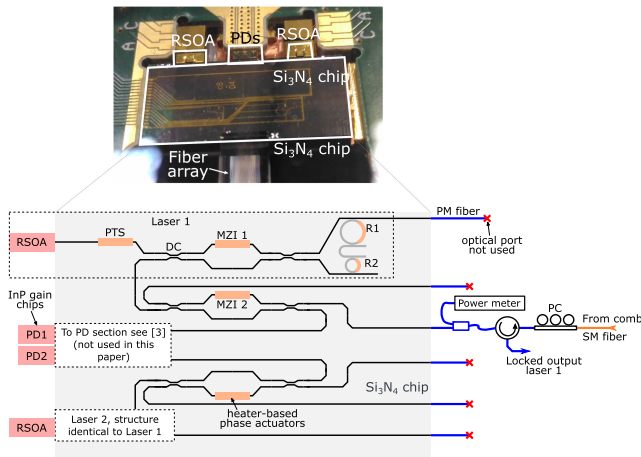


Fig. 1. Image of the hybrid module and schematic representation of it together with the experimental setup used to couple the light in and out of the photonic circuit.

dual-laser PIC to an external modulation-based comb generator. Both real-time and DSP-aided data transmissions are reported at this frequency, achieving, respectively, 12.5 and 28 Gbit/s.

## II. INJECTION LOCKING CHARACTERIZATION

### A. Device Structure

Fig. 1 shows the hybrid circuit forming the dual-laser source. This source has been previously used for free-running mm-wave generation [3] and optical transmission [13]. Since both lasers in the PIC are identical, only the locking characteristics of laser 1 were measured. Each laser integrates an InP quantum-well gain chip and a TriPleX (proprietary  $\text{Si}_3\text{N}_4$  waveguide technology from LioniX International) chip. One of the cavity mirrors is formed by the left edge of the InP chip, which has a high-reflective coating. The other mirror is based on a  $\text{Si}_3\text{N}_4$  double ring resonator. The rings on this resonator have circumferences of  $787.12 \mu\text{m}$  (R2) and  $813.34 \mu\text{m}$  (R1) giving free spectral ranges of 1.72 and 1.67 nm, respectively. Both R1 and R2 have heater-based phase actuators for wavelength tuning. The rest of the cavity is formed by a Mach-Zehnder interferometer (MZI 1) that controls the light that is coupled out of the cavity and a phase tuning section (PTS) that allows fine tuning of the cavity length for output power maximization [14]. Outside the laser cavity there is another MZI (MZI 2) that controls the amount of laser light that is directed to a couple of integrated photodiodes, PDs (which were not used in the experiments reported here) or to the output fiber.

To characterize its comb demux properties, three different OIL measurements were carried out on laser 1: SMSR vs comb spacing (Section II-B), locking range (Section II-C), and SMSR vs offset between comb and laser (Section II-D). For all these measurements, the optical frequency comb was generated with a single phase modulator. As the linewidth of the ECL feeding such a modulator was higher than that of the hybrid laser, the optical linewidth of the latter was deteriorated upon OIL. This is not a problem, however, for optical heterodyne RF generation since the two OIL-filtered comb lines remain coherent and a

very stable mm-wave signal can be generated regardless of the optical linewidths of these lines.

All the results in the sections mentioned before were obtained for a gain current of 180 mA and 18.6 V applied to MZI 2 for cross operation (i.e., no laser light was directed to the PD section). The rest of the phase actuators were not biased. Only a very small bias was applied simultaneously to R1 and R2 in the SMSR-vs-offset characterization. With these settings, the hybrid laser emitted at a wavelength close to 1550 nm, generated an output power of 12.5 dBm, and had a Lorentzian linewidth of 2.9 kHz (see appendix A).

The free-running drift of laser 1 was also characterized (Section II-E). In this case, different bias voltages were applied to the heaters on R1 and R2 to see the effect of temperature on the drift. The PIC is assembled on a thermally-controlled mount through a Peltier thermoelectric cooler (TEC) and NTC thermistor. The module is operated at  $20^\circ\text{C}$  throughout all the reported measurements.

As shown in Fig. 1, the  $\text{Si}_3\text{N}_4$  chip was concertized with an array of polarization maintaining (PM) fibers. To align the polarization of the OFCG output with that of the PM fibers, a polarization controller together with a power meter after a PM 99/1 splitter was used. The light was coupled in and out using the same optical port through a PM circulator.

### B. SMSR vs Comb Spacing

The experimental arrangement used for SMSR characterization is shown in Fig. 2(a). It consisted on the OFCG, a circulator, and a Brillouin-based high resolution optical spectrum analyzer (BOSA). The power and frequency of the RF synthesizer driving the comb was adjusted to generate three lines with equal amplitude and the desired spacing. Fig. 2(b) shows the generated comb spectrum for a line spacing of 15 GHz. To ensure that there was no frequency offset between the 0<sup>th</sup>-order comb sideband and the free-running hybrid laser, the OFCG seed laser was tuned to match the emission wavelength of the latter as shown in Fig. 2(c).

Fig. 2(d) shows the SMSR of the filtered comb line vs comb spacing for different levels of injection ratio, which is defined as the ratio between the power of the single comb line used for locking and that from the hybrid laser in free-running mode. As can be seen, the SMSR decreases as the injected power is increased. This occurs because the power in the side modes increases proportionally with the injected power but the power in the locked line remains constant (approximately equal to the free-running power).

In Fig. 2(d), other SMSR values from OIL-based comb filters reported in the literature are plotted as well. The injection ratio used in these experiments, if available, has also been included in parenthesis with units of dB. None of the cited papers include a continuous sweep of the comb spacing in the characterization of the SMSR and most of them only report the SMSR achieved for a single comb line separation, this is why the data in Fig. 2(d) associated to references [6] to [11] appears as single data points rather than continuous lines. From the papers considered, the only references that provide an SMSR characterization for several comb spacing values are references [6] and [8]. In reference [6],

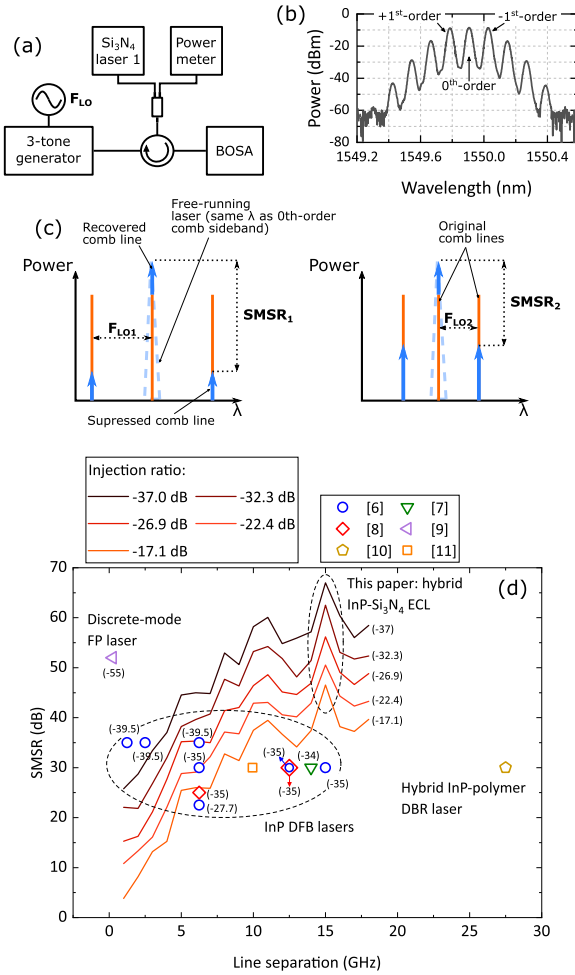


Fig. 2. (a) Measurement arrangement for SMSR characterization; (b) schematic diagram of the optical spectrum obtained before and after locking for different SMSRs; and (c) measured SMSR as a function of comb line separation for zero-frequency detuning between locking line and hybrid laser and different injection ratios.

the SMSR is characterized for an InP distributed feedback (DFB) laser and five different values of comb spacing (1.25, 2.5, 6.25, 12.5 and 15 GHz). The results in this reference (plotted with blue circles in Fig. 2(d)) seem to indicate the SMSR only depends on injection ratio and not in comb spacing. However, this does not appear to be a general trend for InP DFB lasers as the SMSR of the DFB laser reported in [8] (red diamonds in Fig. 2(d)) degrades 5 dB when the comb line separation is reduced from 12.5 to 6.25 GHz. This is more in line with the results reported here, although the SMSR exhibited by the hybrid laser appears to have a stronger frequency dependency.

In any case, above a frequency of around 5 GHz, the hybrid laser exhibits SMSR values well in excess of those previously reported in the literature. As the SMSR depends on the level of comb signal reflected from the slave laser, the higher SMSR values reported here are likely associated to the additional filtering that the reflected signal encounters in the hybrid laser compared to standard DFBs. This additional filtering arises from the multiple round trips that the signal undergoes in the two ring resonators, which yield a longer resonant cavity with a higher

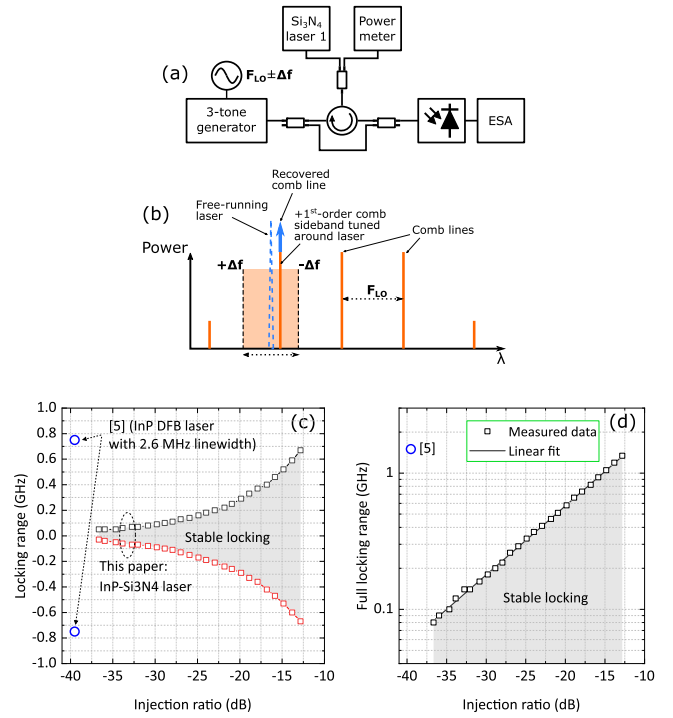


Fig. 3. (a) Measurement arrangement for locking range characterization; (b) schematic diagram of the optical spectrum obtained before and after locking; and (c) measured half and (d) full locking ranges as a function of injection ratio.

$Q$  factor. The  $Q$  factor of the laser cavity has been shown to improve the SMSR of the OIL [5], [12]. Although the  $Q$  factor of the cold hybrid cavity has not been measured directly, based on the measured Lorentzian linewidth (2.9 kHz – see appendix A) and the locking range (see Section II-C) of the InP-Si<sub>3</sub>N<sub>4</sub> laser, its  $Q$  factor is likely to be much higher than commercial DFB lasers as that in [6], with a reported linewidth of 2.6 MHz and a much broader locking range.

### C. Locking Range

In the previous section, the seed laser of the comb was tuned so that there was no offset between the 0<sup>th</sup>-order sideband of the comb and the free-running hybrid laser. OIL, however, allows certain offset between the master and slave laser, which means that, even if the free-running wavelengths of both lasers drift slightly with respect to each other, OIL can still be achieved.

To characterize such offset, which is normally referred to as locking range, the experimental arrangement shown in Fig. 3(a) was used. An optical coupler and a photodiode (PD) were used to beat the output from the hybrid laser with that of the comb. In this case, the +1<sup>st</sup>-order comb sideband was tuned (by sweeping the frequency of the synthesizer driving the OFCG) around the hybrid laser, which was kept at a fixed wavelength (see Fig. 3(b)). The resulting beating signal between the OFCG and the laser output was monitored in an electrical spectrum analyser (ESA). When locked was achieved a clean and stable signal at the comb frequency ( $F_{LO} \pm \Delta f$ ) was visible at the ESA. When the hybrid laser was outside the locking range, numerous intermodulation products appeared at the ESA.

Fig. 3(c) and (d) show the half and full locking ranges, respectively, of the hybrid laser. The latter is obtained by summing the positive and negative half ranges shown in Fig. 3(c). The full locking range is proportional to the square root of the injection ratio [15]. This means that, in a log-vs-10log plot as the one in Fig. 3(d), a slope of 0.05 should be obtained when plotting the locking range. The slope of the linear fit in Fig. 3(d) was calculated to be  $0.0506 \pm 3 \cdot 10^{-4}$ , which matches the theoretical value.

The full locking range of the hybrid laser is substantially lower than that in InP lasers. As an example, the full locking range of the InP DFB laser characterized in [6] (with a linewidth of 2.6 MHz) is 1.5 GHz for an injection ratio of  $-39.5$  dB. On the other hand, for the hybrid laser (linewidth of 2.9 kHz), a locking range of 1.34 GHz was measured for an injection ratio of  $-12.82$  dB. As can be inferred, the locking range decreases with  $Q$  factor.

Typically, a wider locking range is preferred because it enables injection locking over larger drifts between the reference laser and the locked laser. Although this can be achieved by increasing the injected ratio, this will also lead to a reduced SMSR as shown in Fig. 2(d). Hence, to maximize the SMSR, the injection ratio should be the lowest one yielding a locking range wide enough to track the relative drift between the reference and locked lasers. Therefore, one must measure the relative drift between these two lasers in order to estimate the minimum injection ratio required. The free-running drift of laser 1 is reported in Section II-E.

#### D. SMSR vs Offset

After measuring the locking range, the SMSR was characterized again but this time for different offsets between comb and hybrid laser. For this, the setup shown in Fig. 4(a) was used. Different offsets were obtained by tuning the hybrid laser around the 0<sup>th</sup>-order comb line as shown in Fig. 4(b) and each offset was achieved by using the heater-based phase actuators in R1 and R2. Fig. 4(c), (d), (e), and (f) show the SMSR as a function of the comb-hybrid laser frequency offset for comb line separations of 3, 6, 9 and 18 GHz respectively, and two different injection ratios:  $-17$  and  $-32$  dB. In most cases, the SMSR stays constant with offset frequency. This is in contrast to the work reported in [6], where the authors – with reference to a DFB laser with a Lorentzian linewidth of 2.6 MHz – report a strong SMSR degradation with offset frequency. The flatter curves obtained in this paper are attributed to the lower locking range of the hybrid laser and its sharper filtering response.

#### E. Free-Running Drift

As said in Section II-C, measuring the free-running drift of the hybrid laser is key as it determines the minimum locking range (and, hence, injection ratio) required to maintain the OIL. By using the experimental arrangement shown in Fig. 5(a), the drift of laser 1 was measured for different bias configurations on the heaters of R1 and R2. Fig. 5(b), (c), and (d) show the drift measured when only R1 was biased, when only R2 was biased, and when R1 and R2 were simultaneously biased with the same voltage level, respectively. In each of the cases, the

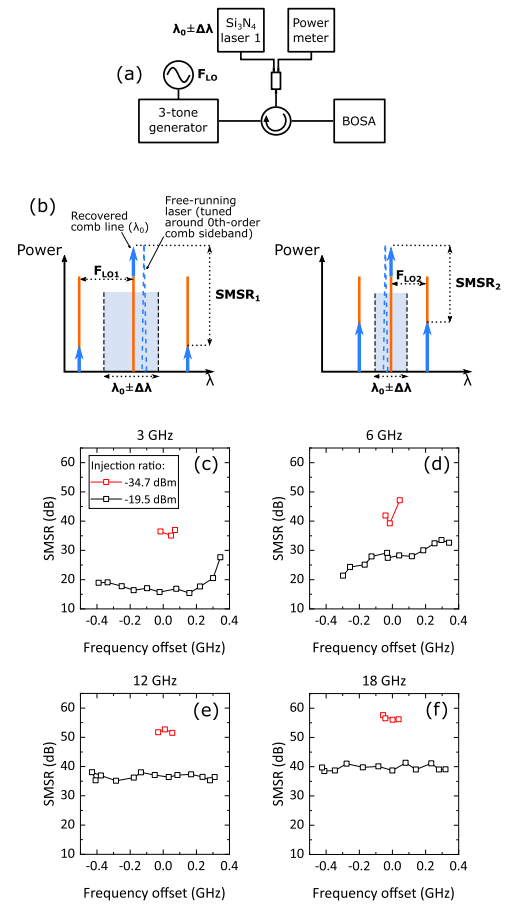


Fig. 4. (a) Measurement arrangement for SMSR vs offset characterization. (b) schematic diagram of the optical spectrum obtained before and after locking for different SMSRs and offsets; and SMSR as a function of the frequency offset between comb and laser for (c) 3 GHz, (d) 6 GHz, (e) 12 GHz, and (f) 18 GHz comb line separations.

voltage level was increased in steps of 2 V from 2 V to 12 V. Some of the curves are not shown in Fig. 5 because, for those particular configurations, either the emission wavelength was outside the BOSA bandwidth or because the laser generated multiple modes.

As can be seen, the drift does not increase with higher voltage levels and, over the measured period of 90 min, all configurations exhibited a drift below  $\pm 60$  MHz. If the OFCG was generated with an identical hybrid laser, the master-slave laser system would have a combined drift of less than  $\pm 120$  MHz. This translates into a required full locking range of 240 MHz, which, according to Fig. 5(d), is achieved with an injection ratio of  $-27$  dB. With this injection ratio, a SMSR higher than 45 dB can be achieved at comb spacings higher than 9 GHz as shown in Fig. 2(d). This is more than 10 dB higher than previously reported values from InP lasers.

Before concluding this section it is important to say that, even if the thermal drift between the master and slave laser is maintained within the locking range, a control loop will always be necessary for practical applications [5]. This is because changes in the wavelength offset between master and slave cause changes in the relative phase between them [5]. In comb demux

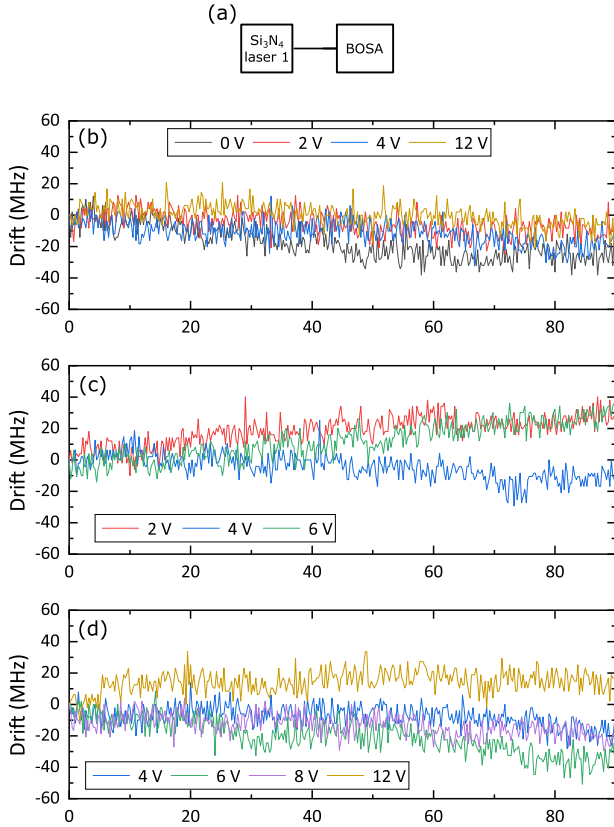


Fig. 5. (a) Experimental arrangement for drift characterization, and drift measured when: (b) only R1 was biased, (c) only R2 was biased, and (d) R1 and R2 where simultaneously biased with the same voltage level.

applications for high-purity RF generation, is essential that these changes are minimized to avoid introducing phase noise between the two filtered tones.

### III. 90-GHZ GENERATION

Three different heater-bias configurations were tried on R1 and R2 of the two lasers in order to set a frequency difference between them of around 90 GHz. The drift associated with each configuration was measured using the arrangement shown in Fig. 6(a). The results of these measurements, together with the biasing details of each configuration are shown in Fig. 6(b). As can be seen, in all configurations, one of the lasers remains very stable while the other exhibits a notable drift. The fact that this drift is suffered by the laser with the lowest biasing levels in each configuration, together with the fact that positive drifts mean cooling, suggests that the Peltier – trying to compensate the heat dissipated by the laser with higher voltage levels – was the responsible of such drift. This agrees with the fact that the drift in Fig. 6(b) increases with the biasing level of the paired laser.

Based on the results of Fig. 6(b) and those in Fig. 5(b), (c), and (d), it seems that the ideal solution is to have independent temperature control for each laser. However, this might increase notably the complexity of the system. Alternatively, designing the dual-laser source to have an initial (i.e., for no applied bias)

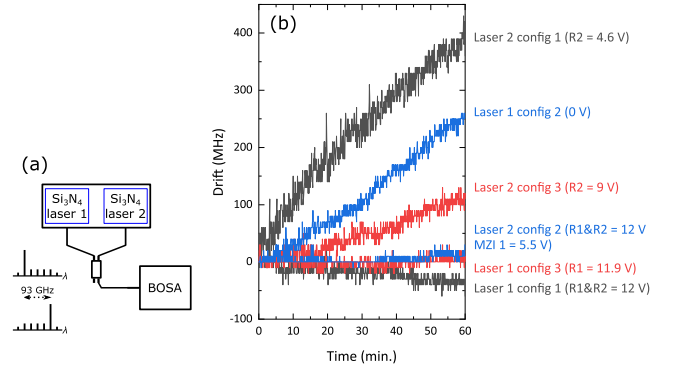


Fig. 6. (a) Arrangement used for dual-laser drift characterization; and (b) drift characterization of the dual-laser source with three different bias configurations to achieve a frequency difference between the two lasers of 90 GHz.

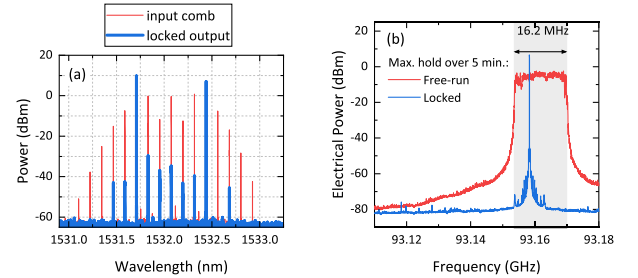


Fig. 7. (a) Input comb and locked output spectra, and (b) max.-hold power spectrum over 5 minutes of the free-running and locked signals.

frequency difference between the two lasers very close to the intended one, so that the biasing load difference between the two lasers is minimized, might be another possible route to decrease the drift shown in Fig. 6(b). It is important to mention that the large voltage levels required in at least one of the lasers in all three configurations employed in this paper are because the initial wavelength offset between the two lasers of the characterized module was around 50 nm. It is believed that reducing this initial offset and making it as close as possible to the required offset for wireless generation (by careful design of the laser cavities) will help decrease the drift.

As it exhibited the lowest amount of drift among the three configurations, config. 3 was chosen for the heterodyne generation. The same optical frequency comb as that in the previous section was used as the external reference. The comb line spacing was set to 15.5 GHz, with the two hybrid lasers locking to the + and  $-3^{\text{rd}}$ -order sidebands, giving a heterodyne frequency of 93.16 GHz. The spectrum of the injected comb, and that of the locked output are shown in Fig. 7(a). The estimated injection ratio for laser 1 and laser 2 was  $-17.8$  dB and  $-16.5$  dB, respectively. According to Fig. 2(d), this injection ratio should give an SMSR of around 40 dB, which seems to be consistent with Fig. 7(a).

Fig. 7(b) shows the obtained max.-hold spectrum for the free-running and OIL heterodyne signals after a period of five minutes. Using a resolution bandwidth of 10 kHz in the ESA, no drift was observed from the locked signal over this period. The ultra-stable properties of the OIL-based signal are inherited

from the phase noise characteristics of the OFCG RF synthesizer, which are shown in appendix B. On the other hand, the max.-hold spectrum from the free-running source stretched over more than 16 MHz. This would already violate the International Telecommunications Union (ITU) current regulation on the stability of mm-wave signals, which specifies a maximum drift of 14 MHz at a carrier frequency of 93 GHz [4]. Thus, even if dealing with ultra-narrow linewidth lasers (the Lorentzian linewidth of the free-running 93-GHz signal under config. 3 was measured to be 4.2 kHz – see appendix A) a locking technique is likely to be required for practical applications.

#### IV. COMMUNICATION EXPERIMENTS

In this section, the results of two communication experiments carried out with the dual-laser hybrid source under OIL are reported. The receiver used in these experiments is an envelope detector (ED), which is insensitive to phase noise and, thus, can be used to recover jittery signals (which may have either real symbols or complex ones as shown in [16]). Using this detector, hence, one would expect to see no difference in performance between a locked source and a free-running source. The claim that is made here for using such a detector with a locked source is that even systems based on EDs will need an ultra-stable wireless signal to comply with ITU stability regulations as discussed in the previous section. Thus, we envisage the use of the high-purity source + ED system reported here in all those cases where minimizing the cost of the receiver is key. This is the case, for example, in mobile terminals, where the use of an ED minimizes power consumption and complexity as no LO is required.

Two different transmission experiments at 93 GHz are reported in this section: a real-time transmission of 12.5-GBd on-off keying (OOK) signals, and a DSP-aided transmission of 7-GBd 16-quadrature amplitude modulation (QAM) signals. For the two experiments, a gain current of around 180 mA was used in both lasers, each of them generating an output power of 12.5 dBm. The same injection ratios as those in Section III (i.e., around  $-17$  dB) were used, giving an SMSR of approximately 40 dB in each laser.

##### A. 93-GHz Real-Time Transmission

The experimental arrangement for real-time transmission is shown in Fig. 8(a). The output of the OFCG was split in a 50/50 coupler and sent to the module containing the two hybrid lasers via two circulators. After optical combination of the OIL output of both lasers, a Mach-Zehnder modulator (MZM) was used to encode a sequence of 12.5-GHz nonreturn-to-zero (NRZ) pulses in both lasers. The modulated signals (whose spectrum is shown in Fig. 8(b)) were then amplified and injected into an F-band waveguide-coupled uni-traveling carrier photodiode (NTT IOD-PMF-13001).

The 93-GHz signal was then launched into free space with a horn antenna and collimated with a Teflon lens. At the receiver side, another identical Teflon lens focused the 93 GHz signal into an envelope detector (ED) [17]. This ED has a Si lens for light coupling, and, hence, is not subjected to the frequency limitations imposed by waveguide-based components. After the ED, low-noise and limiting amplification were applied to the

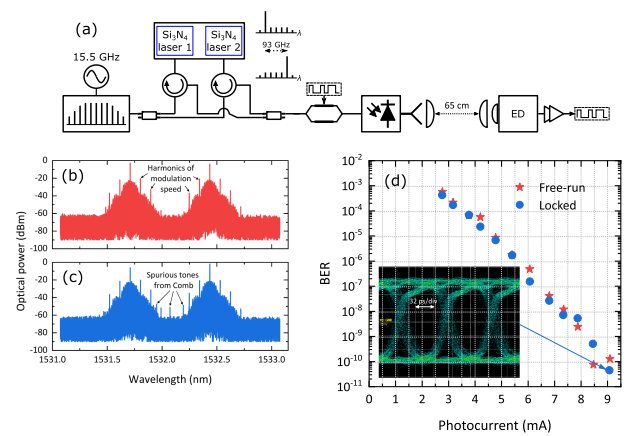


Fig. 8. (a) Experimental arrangement for real-time transmission at 93 GHz; optical spectrum after Mach-Zehnder modulator (MZM) for (b) free-running and (c) locked signals; and (d) bit error rate (BER) curves of the free-running and locked signals.

signal before it was sent to a bit error tester (BERT), where eye diagram analysis and bit error counting were carried out. Transmission experiments were performed at the maximum speed of the BERT – 12.5 Gbit/s.

In this experiment, the performance of the dual-source in locked mode was compared with that of the same source in free-running mode. As discussed before, one would expect a similar performance from the two schemes. However, it is important to realize that, when the source is operated in locked mode, the unwanted OFCG tones that are not totally suppressed by the OIL-based filter leak into the PD. These tones beat with the useful signal and can cause distortion. In [10], where a similar experiment is reported with two polymer lasers locked to an external comb, these spurious tones are cited as the main reason limiting the data speed of the system. On the other hand, when the hybrid source is operated in free-running mode, no spurious tones from the OFCG are present and a cleaner signal is injected into the PD (this can be seen in Fig. 8(b) and (c), which show the optical spectrum at the input of the PD for the free-running and locked signals, respectively). Since no spurious tones are present in the free-running signal, its performance can be taken as an upper limit for that of the locked signal. So, the comparison between schemes is employed here to see how well the hybrid laser was suppressing the unwanted OFCG tones. In Fig. 8(c), the BER curves from the two transmission schemes are plotted as a function of the photocurrent in the UTC-PD. As can be seen, an identical performance between the free-running and locked transmissions was achieved. This suggests that the SMSR achieved by the hybrid source (around 40 dB) is enough to avoid distortion from the spurious tones and confirms the quality of the locking.

##### B. 93-GHz DSP-Aided Transmission

The fact that the ED is insensitive to phase noise does not mean it cannot recover phase-multiplexed signals as shown in [16]. To extend the data rate of the system presented in Section IV-A, a DSP-aided transmission of a 16-quadrature

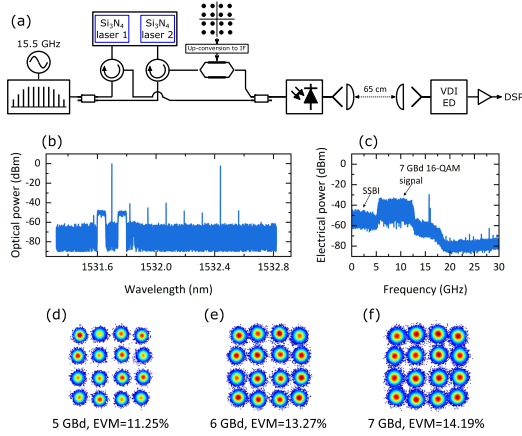


Fig. 9. (a) Experimental arrangement for DSP-aided transmission at 93 GHz; (b) optical spectrum of the UTC input signal; (c) electrical spectrum of the digitized signal in the oscilloscope; and (d), (e), and (f) constellation diagrams of the 16-QAM demodulated signals for symbol speeds of 5, 6, and 7 GBd, respectively. SSBI: signal-to-signal beat interference.

amplitude modulation (QAM) signal was performed. The experimental arrangement used for such transmission is shown in Fig. 9(a). In this case, the ED was a waveguide-coupled ED from VDI (WR10ZBD-F), with a slightly better sensitivity at 93 GHz than the one in Section IV-A. Also, as shown in Fig. 9(a), only the output of laser 1 was modulated. Digital-to-analog and analog-to-digital conversion were performed with a Keysight arbitrary waveform generator (M8195 A) and oscilloscope (UXR0334 A), respectively. Only low-noise amplification was applied in this case to the recovered signal before digitalization.

A conventional DSP routine was used for data generation and reception with the only difference that no frequency offset or phase noise compensation algorithms were required at the receiver due to the high purity of the transmitted signal. A guard-band between the optical carrier and data-carrying signal was intentionally set (as can be seen from Fig. 9(b)) to reduce the signal-signal beat interference (SSBI). Fig. 9(c) shows the spectrum of the signal digitised by the oscilloscope. The peak at 15.5 GHz is caused by the spurious tones from the OFCG adjacent to the data-carrying signals. Fig. 9(d), (e), and (f) show the 16-QAM constellation diagrams for symbol rates of 5, 6, and 7 GBd, respectively.

A data speed of up to 28 Gbit/s (corresponding to the symbol rate of 7 GBd) was successfully transmitted over the wireless link. The main limitations of the current system are two: the bandwidth of the low-noise receiver amplifier – 12 GHz – and the dynamic range of the MZM driver amplifier. The limited bandwidth of the LNA, together with the need for a guard-band to combat the SSBI made it difficult to transmit at speeds faster than 7 GBd. On the other hand, the MZM driver amplifier introduced non-linear distortions for relatively low AWG output powers. Because of this, the modulator was driven with a peak-to-peak voltage substantially lower than half of its  $\pi$  voltage (from Fig. 9(b) one can see that the modulation index was rather low).

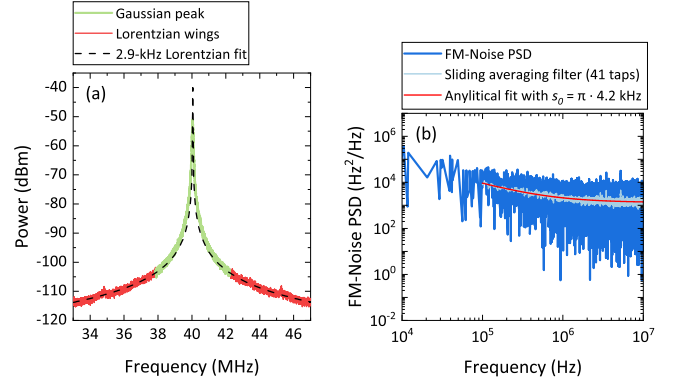


Fig. 10. (a) Electrical spectrum of the hybrid laser obtained with the self-heterodyne technique, and (b) FM noise of the beating between the two hybrid lasers.

## V. CONCLUSION

The optical injection locking characteristics of a hybrid InP-Si<sub>3</sub>N<sub>4</sub> laser when used as an active comb demux filter with power boosting capabilities have been characterized. While the adjacent-comb-line SMSR is measured to be higher than values previously reported from InP DFB lasers, the locking range is substantially lower than that from these lasers. However, based on the reported characterization, it is shown how locking ranges of  $\pm 120$  MHz could be enough in systems where both the comb seed laser and the locked lasers are realized with the hybrid InP-Si<sub>3</sub>N<sub>4</sub> laser presented here. This locking range can be achieved with an injection ratio of  $-27$  dB, which has an associated SMSR of more than 45 dB for comb spacings higher than 9 GHz. Successful carrier generation at 93 GHz is demonstrated by locking two integrated hybrid InP-Si<sub>3</sub>N<sub>4</sub> lasers to an optical frequency comb achieving an ultra-stable ITU-compliant signal. Both real-time and DSP-aided data transmissions are achieved at this frequency with data rates of 12.5 and 28 Gbit/s, respectively.

## APPENDIX A

### OPTICAL AND RF FREE-RUNNING LINewidth MEASUREMENTS

The intrinsic linewidth of laser 1 with the bias settings used throughout Section II was measured using the self-heterodyne technique. The power spectrum obtained from such a laser is shown in Fig. 10(a). A 2.9-kHz linewidth was estimated by using only the wings of the spectrum for Lorentzian fitting in order to avoid distortion by the Gaussian peak and the noise floor [1].

The Lorentzian linewidth of the free-running RF signal at 93 GHz was also measured. As different bias settings of the lasers can produce different phase noise characteristics [3], it was important to measure the signal using the same heater bias configuration employed during the experiments. In order to downconvert the phase noise characteristics of the 93-GHz signal to a frequency within the oscilloscope bandwidth (33 GHz), optical downconversion through comb generation was used. This was achieved by sending the output of laser 2 to a phase modulator (PM), where several replicas with the same phase noise characteristics as laser 2 (assuming the phase noise

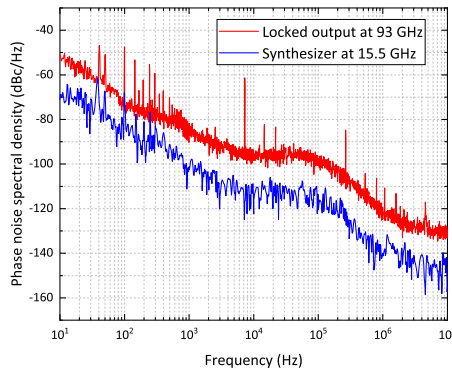


Fig. 11. Phase noise spectral density of the 93-GHz locked signal and that from the 15.5-synthesizer signal used to drive the OFCG.

of the PM RF synthesizer is negligible compared to that of the laser) were generated. Laser 1 was then mixed with the 5<sup>th</sup>-order modulation comb sideband from laser 2 using a 50-GHz PD. The electrical output was recorded in the oscilloscope and the power spectral density (PSD) of the frequency-modulation (FM) noise was digitally extracted following the steps detailed in [18]. The Lorentzian linewidth was obtained by analytically fitting the PSD shown in Fig. 10(b) with the following function [19]:

$$\text{FM-PSD}(f) = s_2/f^2 + s_1/f + s_0,$$

where  $s_2$  is the random walk frequency noise component,  $s_1$  is the  $1/f$  noise component, and  $s_0$  is the white frequency noise component, which is equal to the Lorentzian linewidth down-scaled by a factor of  $\pi$ . The measured intrinsic linewidth was 4.2 kHz.

## APPENDIX B PHASE NOISE MEASUREMENTS

The phase noise of the generated 93-GHz locked signal was measured with the ESA to confirm the quality of the locking. Fig. 11 shows the phase noise of the 93-GHz signal and also that from the 15.5-GHz synthesizer signal used to drive the OFCG. As the multiplication factor was 6 (i.e.,  $15.5 \times 6 = 93$ ), the theoretically-expected difference between the two curves is  $20 \cdot \log_{10}(6) = 15.6$  dB, which is approximately the difference observed in Fig. 11.

## ACKNOWLEDGMENT

The authors would like to thank Keysight for lending the AWG and digital oscilloscope used in the DSP-aided transmission.

## REFERENCES

- [1] Y. Fan *et al.*, "Hybrid integrated InP-Si<sub>3</sub>N<sub>4</sub> diode laser with a 40-Hz intrinsic linewidth," *Opt. Exp.*, vol. 28, no. 15, pp. 21713–21728, 2020.
- [2] C. Tsokos *et al.*, "True time delay optical beamforming network based on hybrid InP-Silicon nitride integration," *J. Lightw. Technol.*, vol. 39, no. 18, pp. 5845–5854, Sep. 2021.
- [3] R. Guzman *et al.*, "Widely tunable RF signal generation using an InP/Si<sub>3</sub>N<sub>4</sub> hybrid integrated dual-wavelength optical heterodyne source," *J. Lightw. Technol.*, vol. 39, no. 24, pp. 7664–7671, Dec. 2021.
- [4] *Frequency Tolerance of Transmitters*, ITU-R SM.1045-1, vol. 1, 1997.
- [5] Z. Liu and R. Slavik, "Optical injection locking: From principle to applications," *J. Lightw. Technol.*, vol. 38, no. 1, pp. 43–59, 2020.
- [6] P. D. Lakshmi Jayasimha, A. Kaszubowska-Anandarajah, E. P. Martin, M. N. Hammad, P. Landais, and P. M. Anandarajah, "Characterization of a multifunctional active demultiplexer for optical frequency combs," *Opt. Laser Technol.*, vol. 134, 2021, Art. no. 106637, [Online]. Available: <https://doi.org/10.1016/j.optlastec.2020.106637>
- [7] S. T. Ahmad *et al.*, "Active demultiplexer enabled mmW AROF transmission of directly modulated 64-QAM UF-OFDM signals," *Opt. Lett.*, vol. 45, no. 18, pp. 5246–5249, 2020.
- [8] R. Zhou, T. Shao, M. D. Gutierrez Pascual, F. Smyth, and L. P. Barry, "Injection locked wavelength de-multiplexer for optical comb-based nyquist WDM system," *IEEE Photon. Technol. Lett.*, vol. 27, no. 24, pp. 2595–2598, Dec. 2015.
- [9] D. S. Wu, D. J. Richardson, and R. Slavik, "Selective amplification of frequency comb modes via optical injection locking of a semiconductor laser: Influence of adjacent unlocked comb modes," *Integr. Opt.: Phys. Simul.*, vol. 8781, 2013, Art. no. 87810J.
- [10] G. Carpintero, S. Hisatake, D. De Felipe, R. Guzman, T. Nagatsuma, and N. Keil, "Wireless data transmission at terahertz carrier waves generated from a hybrid InP-Polymer dual tunable DBR laser photonic integrated circuit," *Sci. Rep.*, vol. 8, no. 1, pp. 1–7, 2018. [Online]. Available: <http://dx.doi.org/10.1038/s41598-018-21391-0>
- [11] M. C. Lo *et al.*, "Foundry-fabricated dual-DFB PIC injection-locked to optical frequency comb for high-purity THz generation," in *Proc. Opt. InfoBase Conf. Papers*, 2019, vol. Part F160, pp. 3–5.
- [12] K. Shortiss, M. Shayesteh, W. Cotter, A. H. Perrott, M. Dernaika, and F. H. Peters, "Mode suppression in injection locked multi-mode and single-mode lasers for optical demultiplexing," *Photonics*, vol. 6, no. 1, 2019, Art. no. 27.
- [13] D. Dass *et al.*, "28 Gb/s PAM-8 transmission over a 100 nm range using an InP-Si<sub>3</sub>N<sub>4</sub> based integrated dual tunable laser module," *Opt. Exp.*, vol. 29, no. 11, pp. 16563–16571, 2021.
- [14] K. J. Boller *et al.*, "Hybrid integrated semiconductor lasers with silicon nitride feedback circuits," *Photonics*, vol. 7, no. 1, 2020, Art. no. 4.
- [15] Y. Fan *et al.*, "Q-factor measurements through injection locking of a semiconductor-glass hybrid laser with unknown intracavity losses," *Opt. Lett.*, vol. 39, no. 7, pp. 1748–1751, 2014.
- [16] M. F. Hermelo, P.-T. B. Shih, M. Steeg, A. Ng'oma, and A. Stöhr, "Spectral efficient 64-QAM-OFDM terahertz communication link," *Opt. Exp.*, vol. 25, no. 16, pp. 19360–19370, 2017.
- [17] M. Ali, R. C. Guzman, A. Rivera-Lavado, O. Cojocari, L. E. Garcia-Muñoz, and G. Carpintero, "Quasi-optical schottky barrier diode detector for mmWave/sub-THz wireless communication," in *Proc. 25th Int. Conf. Telecommun.*, 2018, pp. 279–282.
- [18] L. Gonzalez-Guerrero *et al.*, "Pilot-tone assisted 16-QAM photonic wireless bridge operating at 250 GHz," *J. Lightw. Technol.*, vol. 39, no. 9, pp. 2725–2736, 2021.
- [19] I. Fatadin, D. Ives, and S. J. Savory, "Differential carrier phase recovery for QPSK optical coherent systems with integrated tunable lasers," *Opt. Exp.*, vol. 21, no. 8, 2013, Art. no. 10166. [Online]. Available: <https://www.osapublishing.org/oe/abstract.cfm?uri=oe-21-8-10166>